

Baryon Number Fluctuations in NJL Model

Ameng Zhao^{1*} and Hongshi Zong^{3,4,5}

¹ *Department of Foundation, Southeast University*

Chengxian College, Nanjing 210088, China

³ *Department of Physics, Nanjing University, Nanjing 210093, China*

⁴ *Joint Center for Particle, Nuclear Physics and Cosmology, Nanjing 210093, China and*

⁵ *State Key Laboratory of Theoretical Physics,*

Institute of Theoretical Physics, CAS, Beijing 100190, China

Abstract

Baryon number fluctuations are believed to be good signatures of the QCD phase transition and its CP. Since the fluctuations are proportional to the various order baryon-number susceptibilities and the quark-number density is determined by the dressed quark propagator only, then by the dressed quark propagator of NJL model we can calculate the moments of quark number. We choose the parameterized scheme by J. Cleymans and the recent RHIC results to correspond the freeze-out temperature T and the quark chemical potential μ in NJL results to the collision energies $\sqrt{S_{NN}}$ in experiments. It is found that in the latter case the results of NJL model fit the experimental better, especially in $0 - 5\%$ centrality. At the same time there are still some problems to be noticed: when $\sqrt{S_{NN}} \leq 10\text{GeV}$ the NJL results show obvious fluctuations; the NJL results are comprehensively less than the experimental data; the NJL results behave differently from the experimental data in some cases.

Keywords: baryon number fluctuations, nonlinear susceptibilities, Nambu-Jona-Lasinio(NJL) model.

*Email:zhaoameng@cxxy.seu.edu.cn

I. INTRODUCTION

Lattice QCD calculations indicate that at baryon chemical potential $\mu_B = 0$, the transition from the quark-gluon plasma(QGP) to a hadron gas is a smooth crossover, while at large μ_B , the phase transition is of first order. And the first order transition ends at a critical point(CP), which the RHIC experiments suggest is unlikely to below $\mu_B = 200$ MeV[1]. To search for the CP and phase boundary in the QCD phase diagram, RHIC has undertaken its first phase BES(Beam Energy Scan) Program[2–6]. Since the moments of the distributions of conserved quantities, for example net-baryon number, in the relativistic heavy ion collisions are related to the correlation length ξ of the system[7, 8], they are believed to be good signatures of the QCD phase transition and its CP.

It is known that the moments of the baryon number are proportional to the various order baryon-number susceptibilities, and their relations are shown in [9]. It can be seen that when relating the susceptibilities to the moments a volume term appears. In order to cancel the volume term, the products of the moments, $S\sigma$ and $\kappa\sigma^2$, are constructed as the experimental observables. The results in RHIC of these observables show a centrality and energy dependence[10]. When studying the quark numbers at finite temperature and chemical potential, it is found that the quark-number density is determined by the corresponding dressed quark propagator only[11, 12]. Then by calculating the derivatives of the quark-number density with respect to μ , we can calculate the quark-number susceptibilities at finite temperature and chemical potential.

In this paper, we obtain the dressed quark propagator in the Nambu-Jona-Lasinio(NJL) model. The NJL model[13–15], as a widely adopted phenomenological model of QCD, is used to study the dynamical chiral symmetry breaking(DCSB) and the interaction between hadrons. The NJL model keeps the basic symmetries of QCD and simplifies the interactions in QCD to four-body interactions.

II. MOMENTS BY NJL MODEL

The commonly used Lagrangian of the two-flavor NJL model is

$$\mathcal{L} = \bar{\psi}(i\gamma^\mu\partial_\mu - m)\psi + G[(\bar{\psi}\psi)^2 + (\bar{\psi}i\gamma_5\vec{\tau}\psi)^2], \quad (1)$$

where $m = m_u = m_d$, $\psi = (\psi_u, \psi_d)^T$ and G is the effective coupling strength of the four-point quark interaction. With the mean field approximation of Eq.1, the effective quark mass M is

$$M = m - 2G < \bar{\psi}\psi >, \quad (2)$$

where the quark condensate at finite temperature(T) and chemical potential(μ) is defined as

$$\begin{aligned} < \bar{\psi}\psi > = -TN_c N_f \sum_{-\infty}^{+\infty} \int^{\Lambda} \frac{d^3p}{(2\pi)^3} \frac{4M}{p^2 + M^2 + \tilde{\omega}_n^2} \\ &= -\frac{N_c N_f M}{2\pi^2} \int^{\Lambda} dp \frac{p^2}{\sqrt{p^2 + M^2}} \left(th\left(\frac{\sqrt{p^2 + M^2} + \mu}{2T}\right) + th\left(\frac{\sqrt{p^2 + M^2} - \mu}{2T}\right) \right), \end{aligned} \quad (3)$$

where $N_c = 3$ is the number of color and $N_f = 2$ is the number of flavor, $\tilde{\omega}_n = 2\pi nT + i\mu$ and the NJL model three-momentum non-covariant cut-off is Λ . In this paper, we adopt a varying coupling strength G [16–20], which is used to reproduce the Lattice results at finite temperature[19, 20]:

$$G = G_1 + G_2 < \bar{\psi}\psi >, \quad (4)$$

where G in the NJL model represents the effective gluon propagator, $G_2 < \bar{\psi}\psi >$ reflects the contribution of the two-quark condensate to the gluon propagator and G_1 reflects all the other condensate contributions. Since the quark propagator and gluon propagator are coupled with each other by QCD and the quark propagator in Nambu and Wigner phase are very different, then the corresponding gluon propagators in these two phases should be different too. At the same time Lattice results have shown that the gluon propagator, rather than a constant, evolves with temperature. That is to say a constant G does not meet these requirements. In [19] they investigate how to extract the feedback of quark from gluon propagator and get Eq.4. The parameter set used in this paper is $m = 5.6MeV$, $\Lambda = 587.9MeV$, $G_1 = 5.564 \times 10^{-6}MeV^{-2}$ and $G_2 = -3.16 \times 10^{-14}MeV^{-5}$, which is proved to be successful in fitting the quark condensate to the Lattice results at finite temperature[20]. Then by Eq.2 we could get the effective quark mass M as a function of T and μ . Since the

quark number density of N_c color and N_f flavor is[11, 12]

$$\begin{aligned}
n_q &= \langle \psi^\dagger \psi \rangle = -TN_c N_f \sum_{-\infty}^{+\infty} \int \frac{d^3 p}{(2\pi)^3} T_r[G(p, \mu) \gamma_4] \\
&= TN_c N_f \sum_{-\infty}^{+\infty} \int \frac{d^3 p}{(2\pi)^3} \frac{4i\tilde{\omega}_n}{p^2 + M^2 + \tilde{\omega}_n^2} \\
&= \frac{TN_c N_f}{\pi^2} \int dp \cdot p^2 \sum_{-\infty}^{+\infty} \left(\frac{1}{\epsilon - (i\omega_n - \mu)} - \frac{1}{\epsilon + (i\omega_n - \mu)} \right) \\
&= \frac{N_c N_f}{\pi^2} \int dp \cdot p^2 \left(\frac{1}{e^{\beta(\epsilon - \mu)} + 1} - \frac{1}{e^{\beta(\epsilon + \mu)} + 1} \right),
\end{aligned} \tag{5}$$

where $\epsilon = \sqrt{p^2 + M^2}$. Then the quark number density of a single color and flavor is

$$n = \frac{1}{\pi^2} \int dp \cdot p^2 \left(\frac{1}{e^{\beta(\epsilon - \mu)} + 1} - \frac{1}{e^{\beta(\epsilon + \mu)} + 1} \right). \tag{6}$$

The variance of baryon number density is

$$\begin{aligned}
\sigma^2 &= \langle (n_B - \langle n_B \rangle)^2 \rangle \\
&= \frac{1}{3^2} \langle (n_q - \langle n_q \rangle)^2 \rangle \\
&= \frac{1}{3^2} \langle [(n_u + n_d) - \langle n_u + n_d \rangle]^2 \rangle \\
&= \frac{1}{3^2} \langle (n_u - \langle n_u \rangle)^2 \rangle + \langle (n_d - \langle n_d \rangle)^2 \rangle \\
&= \frac{N_f}{3^2} \langle (n_f - \langle n_f \rangle)^2 \rangle.
\end{aligned} \tag{7}$$

where n_f represents the quark number density of a single flavor. Since the up quarks and down quarks are independent, as in [21], we have $\langle (n_u - \langle n_u \rangle)(n_d - \langle n_d \rangle) \rangle = 0$ here. And $n_f = n_1 + n_2 + n_3$, where n_1 , n_2 and n_3 represent the quark number density of three different color respectively. Since the confinement nature of QCD, $\langle n_i n_j \rangle = \langle n^2 \rangle$ ($i, j = 1, 2, 3$). Then the variance of n_f is

$$\begin{aligned}
\langle (n_f - \langle n_f \rangle)^2 \rangle &= \langle [(n_1 + n_2 + n_3) - \langle n_1 + n_2 + n_3 \rangle]^2 \rangle \\
&= N_c^2 \langle (n - \langle n \rangle)^2 \rangle,
\end{aligned} \tag{8}$$

and $\langle (n - \langle n \rangle)^2 \rangle$ could be calculate in theory by the relation $\langle (n - \langle n \rangle)^2 \rangle = T \frac{\partial n}{\partial \mu} = T \cdot \chi^{(2)}$. Then with Eq.7, we could get

$$\begin{aligned}
\sigma^2 &= \frac{N_f}{3^2} \langle (n_f - \langle n_f \rangle)^2 \rangle \\
&= \frac{N_f N_c^2}{3^2} \langle (n - \langle n \rangle)^2 \rangle \\
&= N_f \langle (n - \langle n \rangle)^2 \rangle = N_f \cdot \chi^{(2)}.
\end{aligned} \tag{9}$$

Similarly, we could get

$$\begin{aligned}
S\sigma &= \frac{\langle (n_B - \langle n_B \rangle)^3 \rangle}{\langle (n_B - \langle n_B \rangle)^2 \rangle} = \frac{N_f \langle (n - \langle n \rangle)^3 \rangle}{N_f \langle (n - \langle n \rangle)^2 \rangle} \\
&= \frac{T^2 \chi^{(3)}}{T \chi^{(2)}} = T \frac{\chi^{(3)}}{\chi^{(2)}},
\end{aligned} \tag{10}$$

and

$$\begin{aligned}
\kappa\sigma^2 &= \frac{\langle (n_B - \langle n_B \rangle)^4 \rangle - 3 \langle (n_B - \langle n_B \rangle)^3 \rangle}{\langle (n_B - \langle n_B \rangle)^2 \rangle} \\
&= \frac{\langle (n - \langle n \rangle)^4 \rangle - 3 \langle (n - \langle n \rangle)^3 \rangle}{\langle (n - \langle n \rangle)^2 \rangle} \\
&= T^2 \frac{\chi^{(4)}}{\chi^{(2)}}.
\end{aligned} \tag{11}$$

where $\frac{\partial^2 n}{\partial \mu^2} = \chi^{(3)}$ and $\frac{\partial^3 n}{\partial \mu^3} = \chi^{(4)}$. That is to say by calculating the high order derivatives of Eq.6 with respect to μ , we could get the experimental observables $S\sigma$ and $\kappa\sigma^2$ in the relativistic heavy ion collisions.

III. RESULTS

Before comparing the $S\sigma$ and $\kappa\sigma^2$ results of the NJL model with the experimental data in the relativistic heavy ion collisions, we should find the correspondence of the freeze-out temperature T and the quark chemical potential μ in the NJL results to the collision energies $\sqrt{S_{NN}}$ in the relativistic heavy ion collisions.

Firstly, we adopt a parameterized scheme by J. Cleymans and H. Oeschler, etc in Ref.[22]. In the paper they proposed that $T = a - b\mu_B^2 - c\mu_B^4$ and $\mu_B = d/(1 + e\sqrt{S_{NN}})$, where $a = 0.166 \pm 0.002 GeV, b = 0.139 \pm 0.016 GeV^{-1}, c = 0.053 \pm 0.021 GeV^{-3}, d = 1.308 \pm 0.028 GeV, e = 0.273 \pm 0.008 GeV^{-1}$ and $\mu_B = 3\mu$ is the baryon chemical potential. Since each parameter(a,b,c,d,e) have the value range, we demonstrate the upper and the lower limit of the NJL model results in Fig.1 as solid lines. At the same time, the $S\sigma$ and $\kappa\sigma^2$ results[23, 24] of three different centralities(0 – 5%, 30 – 40% and 70 – 80%) at RHIC are shown as filled squares, triangles and circles respectively.

The experimental data in 0 – 5% centrality has a different tendency comparing with the data in 30 – 40% and 70 – 80% centralities. It comes from the fact that the freeze-out temperature T and the baryon chemical potential μ_B in different centralities are different. As

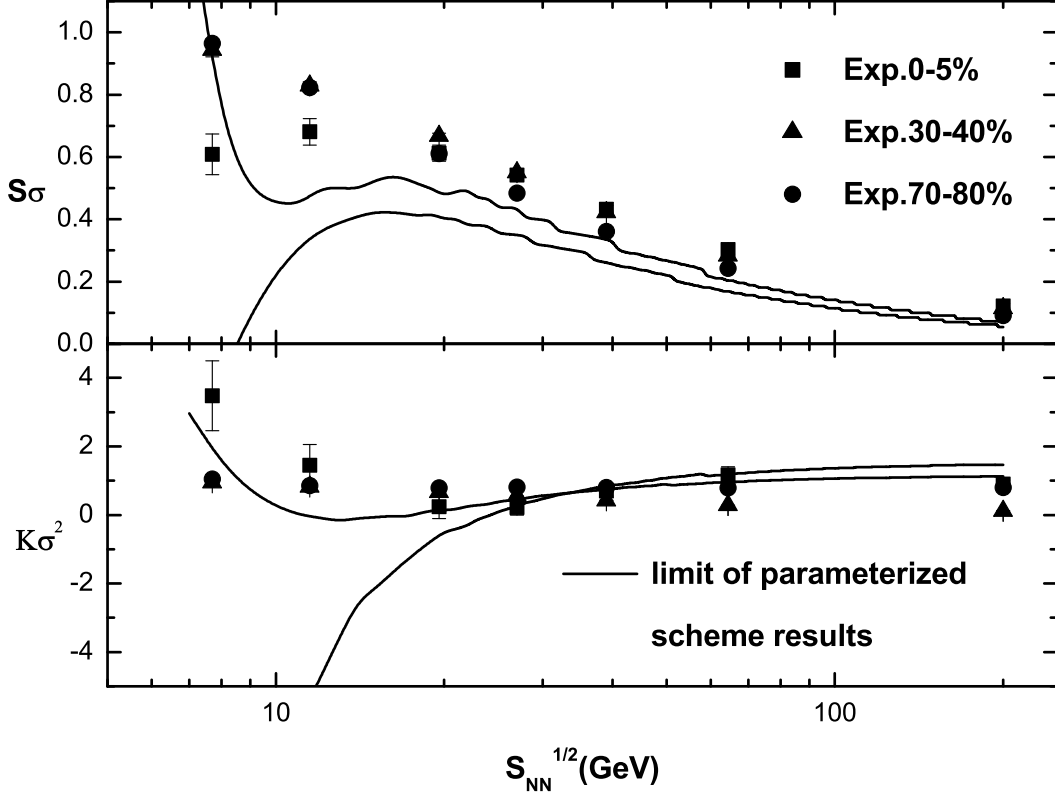


FIG. 1: Solid lines represent the upper and the lower limit of the NJL model results. Data points[23, 24] are the experimental results of $S\sigma$ and $\kappa\sigma^2$ (0–5%, 30–40% and 60–80% centralities).

the experimental data, the upper and the lower limit of the NJL model in Fig.1 demonstrate an obvious deviation when the collision energies $\sqrt{S_{NN}}$ is less than 10GeV. And the deviation narrows when $\sqrt{S_{NN}}$ is more than 20GeV. But the NJL results are comprehensively less than the experimental data of both $S\sigma$ and $\kappa\sigma^2$, except the data of $\kappa\sigma^2$ when $\sqrt{S_{NN}}$ is more than 30GeV.

Secondly, the correspondence of the freeze-out T and μ in the NJL results to the collision energies $\sqrt{S_{NN}}$ comes from the recent experimental results[25]. Since, in Ref.[25], the correspondence is shown in three different centralities (0 – 5%, 30 – 40% and 60 – 80%), then the NJL results of $S\sigma$ and $\kappa\sigma^2$ are also calculated in the three centralities and demonstrate as empty squares, triangles and circles in Fig.2 and Fig.3 respectively. And as in Fig.1, the

experimental results in Ref.[23, 24] are shown as filled patterns.

It could be seen that comparing with it in Fig.1 the NJL result fit the experimental data better in Fig.2 and Fig.3, especially in 0 – 5% centrality the data is in the range of the NJL results basically. And as in Fig.1, the NJL results are comprehensively less than the experimental data, except the results of $\kappa\sigma^2$ during $\sqrt{S_{NN}} \geq 30\text{GeV}$. It is notable that in Fig.2 the $S\sigma$ of experimental data in 30 – 40% centrality show the different tendency from the NJL results. It reflect that at this freeze-out T and μ the NJL model shows different behavior from the experimental data.

In conclusion, the two-flavor NJL model could be used to study the moments of net-baryon distributions in RHIC experiments. And the problems should be noticed are mainly in three aspects. Firstly, when $\sqrt{S_{NN}} \leq 10\text{GeV}$ the NJL results show obvious fluctuations. Secondly, the NJL results are comprehensively less than the experimental data. And at last, the NJL results behave differently from the experimental data in some cases.

IV. SUMMARY

The moments of the distributions of conserved quantities, for example net-baryon number, in the relativistic heavy ion collisions are related to the correlation length ξ of the system[7], they are believed to be the good signatures of QCD phase transition and its CP. In order to cancel the volume term, the products of the moments, $S\sigma$ and $\kappa\sigma^2$, are constructed as the experimental observables. Since the moments of the baryon number are proportional to the various order baryon-number susceptibilities and the quark-number density is determined by the corresponding dressed quark propagator only[11], then by a reasonable dressed quark propagator we can calculate the moments of quark number at finite temperature and chemical potential.

We obtain the dressed quark propagator in the NJL model[13], which is widely adopted to study the dynamical chiral symmetry breaking(DCSB) and the interaction between hadrons. When corresponding the freeze-out temperature T and the quark chemical potential μ in the NJL results to the collision energies $\sqrt{S_{NN}}$ in experiments, we choose the parameterized scheme by J. Cleymans and H. Oeschler, etc and the recent RHIC results[25] at the same time. It is found that in the latter case the results of the NJL model fit the experimental better. Especially in 0 – 5% centrality, the experimental data from RHIC is in the range

of the NJL results basically. Since then it could be concluded that the NJL model is a reasonable choice to study the moments of net-baryon distributions in RHIC.

At the same time there are still some problems to be noticed: when $\sqrt{S_{NN}} \leq 10\text{GeV}$ the NJL results show obvious fluctuations; the NJL results are comprehensively less than the experimental data; the NJL results behave differently from the experimental data in some cases.

Acknowledgements

This work is supported by the University Natural Science Foundation of JiangSu Province China (under Grants No.17KJB140003).

Appendix A

The quark-number density susceptibilities($\chi^{(2)}$, $\chi^{(3)}$ and $\chi^{(4)}$) of a single color and flavor are:

$$\chi^{(2)} = \frac{\partial n}{\partial \mu} = -\frac{1}{\pi^2} \int dp \cdot p^2 \left(\frac{e^s \frac{\partial s}{\partial \mu}}{(e^s + 1)^2} - \frac{e^{s'} \frac{\partial s'}{\partial \mu}}{(e^{s'} + 1)^2} \right), \quad (\text{A1})$$

$$\begin{aligned} \chi^{(3)} = \frac{\partial^2 n}{\partial \mu^2} = & -\frac{1}{\pi^2} \int dp \cdot p^2 \left(\frac{e^s \left(\frac{\partial^2 s}{\partial \mu^2} + \left(\frac{\partial s}{\partial \mu} \right)^2 \right) + e^{2s} \left(\frac{\partial^2 s}{\partial \mu^2} - \left(\frac{\partial s}{\partial \mu} \right)^2 \right)}{(e^s + 1)^3} \right. \\ & \left. - \frac{e^{s'} \left(\frac{\partial^2 s'}{\partial \mu^2} + \left(\frac{\partial s'}{\partial \mu} \right)^2 \right) + e^{2s'} \left(\frac{\partial^2 s'}{\partial \mu^2} - \left(\frac{\partial s'}{\partial \mu} \right)^2 \right)}{(e^{s'} + 1)^3} \right), \end{aligned} \quad (\text{A2})$$

$$\begin{aligned} \chi^{(4)} = \frac{\partial^3 n}{\partial \mu^3} = & -\frac{1}{\pi^2} \int dp \cdot p^2 \left(\frac{1}{(e^s + 1)^4} \left(e^s \left(\frac{\partial^3 s}{\partial \mu^3} + 3 \frac{\partial s}{\partial \mu} \frac{\partial^2 s}{\partial \mu^2} + \left(\frac{\partial s}{\partial \mu} \right)^3 \right) \right. \right. \\ & + e^{2s} \left(2 \frac{\partial^3 s}{\partial \mu^3} - 4 \left(\frac{\partial s}{\partial \mu} \right)^3 \right) + e^{3s} \left(\frac{\partial^3 s}{\partial \mu^3} - 3 \frac{\partial s}{\partial \mu} \frac{\partial^2 s}{\partial \mu^2} + \left(\frac{\partial s}{\partial \mu} \right)^3 \right) \Big) \\ & - \frac{1}{(e^{s'} + 1)^4} \left(e^{s'} \left(\frac{\partial^3 s'}{\partial \mu^3} + 3 \frac{\partial s'}{\partial \mu} \frac{\partial^2 s'}{\partial \mu^2} + \left(\frac{\partial s'}{\partial \mu} \right)^3 \right) \right. \\ & \left. \left. + e^{2s'} \left(2 \frac{\partial^3 s'}{\partial \mu^3} - 4 \left(\frac{\partial s'}{\partial \mu} \right)^3 \right) + e^{3s'} \left(\frac{\partial^3 s'}{\partial \mu^3} - 3 \frac{\partial s'}{\partial \mu} \frac{\partial^2 s'}{\partial \mu^2} + \left(\frac{\partial s'}{\partial \mu} \right)^3 \right) \right) \right), \end{aligned} \quad (\text{A3})$$

where $s = (\epsilon - \mu)/T$ and $s' = (\epsilon + \mu)/T$, that is to say

$$\begin{aligned} \frac{\partial s}{\partial \mu} &= \frac{1}{T} \left(\frac{\partial \epsilon}{\partial \mu} - 1 \right) = \frac{1}{T} \left(\frac{M}{\epsilon} \frac{\partial M}{\partial \mu} - 1 \right) \\ \frac{\partial s'}{\partial \mu} &= \frac{1}{T} \left(\frac{\partial \epsilon}{\partial \mu} + 1 \right) = \frac{1}{T} \left(\frac{M}{\epsilon} \frac{\partial M}{\partial \mu} + 1 \right), \end{aligned} \quad (\text{A4})$$

$$\frac{\partial^2 s}{\partial \mu^2} = \frac{\partial^2 s'}{\partial \mu^2} = \frac{1}{T} \frac{\partial^2 \epsilon}{\partial \mu^2} = \frac{1}{T} \left(\frac{1}{\epsilon} \left(\left(\frac{\partial M}{\partial \mu} \right)^2 + M \frac{\partial^2 M}{\partial \mu^2} \right) - \frac{1}{\epsilon^3} \left(M \frac{\partial M}{\partial \mu} \right)^2 \right), \quad (\text{A5})$$

$$\begin{aligned} \frac{\partial^3 s}{\partial \mu^3} &= \frac{\partial^3 s'}{\partial \mu^3} = \frac{1}{T} \frac{\partial^3 \epsilon}{\partial \mu^3} \\ &= \frac{1}{T} \left(\frac{1}{\epsilon} \left(3 \frac{\partial^2 M}{\partial \mu^2} \frac{\partial M}{\partial \mu} + M \frac{\partial^3 M}{\partial \mu^3} \right) - \frac{3M}{\epsilon^3} \frac{\partial M}{\partial \mu} \left(\left(\frac{\partial M}{\partial \mu} \right)^2 + M \frac{\partial^2 M}{\partial \mu^2} \right) + \frac{3}{\epsilon^5} \left(M \frac{\partial M}{\partial \mu} \right)^3 \right), \end{aligned} \quad (\text{A6})$$

and the value of $\frac{\partial M}{\partial \mu}$, $\frac{\partial^2 M}{\partial \mu^2}$ and $\frac{\partial^3 M}{\partial \mu^3}$ are obtained from the iterative equations

$$\frac{\partial M}{\partial \mu} = -2G_1 \frac{\partial \langle \bar{\psi}\psi \rangle}{\partial \mu} - 4G_2 \langle \bar{\psi}\psi \rangle \frac{\partial \langle \bar{\psi}\psi \rangle}{\partial \mu}, \quad (\text{A7})$$

$$\frac{\partial^2 M}{\partial \mu^2} = -2G_1 \frac{\partial^2 \langle \bar{\psi}\psi \rangle}{\partial \mu^2} - 4G_2 \langle \bar{\psi}\psi \rangle \frac{\partial^2 \langle \bar{\psi}\psi \rangle}{\partial \mu^2} - 4G_2 \left(\frac{\partial \langle \bar{\psi}\psi \rangle}{\partial \mu} \right)^2, \quad (\text{A8})$$

$$\frac{\partial^3 M}{\partial \mu^3} = -2G_1 \frac{\partial^3 \langle \bar{\psi}\psi \rangle}{\partial \mu^3} - 4G_2 \langle \bar{\psi}\psi \rangle \frac{\partial^3 \langle \bar{\psi}\psi \rangle}{\partial \mu^3} - 12G_2 \frac{\partial \langle \bar{\psi}\psi \rangle}{\partial \mu} \frac{\partial^2 \langle \bar{\psi}\psi \rangle}{\partial \mu^2}. \quad (\text{A9})$$

-
- [1] M. M. Aggarwal et al., Phys. Rev. Lett. 105, 022302(2010).
 - [2] B. Abelev et al. (STAR Collaboration), Phys. Rev. C 81, 024911 (2010).
 - [3] B. Mohanty, Nucl. Phys. A 830, 899c (2009).
 - [4] M. Aggarwal et al. (STAR Collaboration), arXiv: p. 1007.2613 (2010);
 - [5] L. Kumar (STAR Collaboration), Nucl. Phys. A 904, 256c (2013).
 - [6] L. Kumar, Mod. Phys. Lett. A 28, 1330033 (2013).
 - [7] M. A. Stephanov, Phys. Rev. Lett. 102, 032301 (2009).
 - [8] C. Athanasiou et al., Phys. Rev. D 82, 074008 (2010).
 - [9] S. Gupta et al., Science 332, 1525 (2011).
 - [10] L. Adamczyk et al., Phys. Rev. Lett. 112, 032302 (2014).
 - [11] H.S. Zong and W.M. Sun, Phys.Rev.D78,054001(2008).
 - [12] M. He, J.F. Li, W.M. Sun and H.S. Zong,Phys.Rev.D79, 036001 (2009).
 - [13] S. P. Klevansky, Rev. Mod. Phys. 64, 649 (1992).
 - [14] M. Buballa, Phys. Rep. 407, 205-376 (2005).
 - [15] H. Kohyama, D. Kimura and T. Inagaki, Nucl. Phys. B 896, 682-715 (2015).
 - [16] Z.F. Cui, C. Shi, Y.H. Xia, Y. Jiang and H.S. Zong, Eur. Phys. J. C 73, 2612 (2013)

- [17] Z.F. Cui , C. Shi , W.M. Sun, Y.L. Wang and H.S. Zong, Eur. Phys. J. C 74, 2782 (2014).
- [18] Q.W. Wang, Z.F. Cui and H.S.Zong, Phys. Rev. D94, 096003 (2016).
- [19] C.M. Li, J.L. Zhang, Y. Yan, Y.F. Huang and H.S. Zong, Phys.Rev. D97 103013 (2018).
- [20] Z.Y. Fan, W.K. Fan, Q.W. Wang and H.S. Zong, Mod. Phys. Lett. A Vol. 32, No. 20 1750107(2017).
- [21] A.M. Zhao, X.F. Luo, H.S. Zong, Eur. Phys. J. C 77:207 (2017).
- [22] J. Cleymans, H. Oeschler, K. Redlich and Pl. Maksa, arXiv:0511094(2008).
- [23] X. Luo, PoS(CPOD2014)019. arXiv: 1503.02558.
- [24] X. Luo, Nucl. Phys. A, 1-9 (2016). arXiv:1512.09215.
- [25] L. Adamczyk et al.(STAR Collaboration),arXiv:1701.07065 (2017).

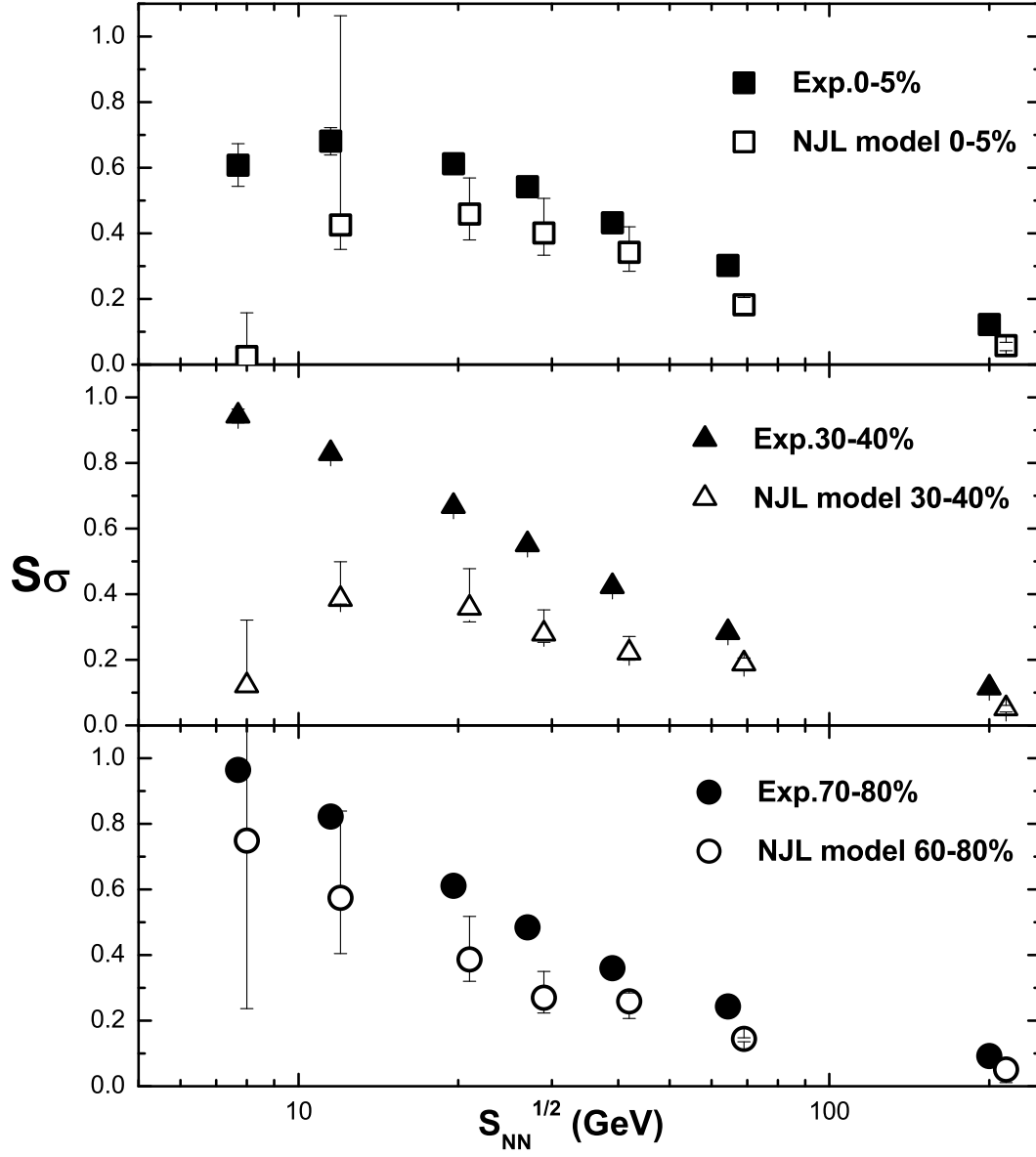


FIG. 2: $S\sigma$ of the NJL model and the experiments. The NJL results demonstrate as empty squares, triangles and circles(0 – 5%, 30 – 40% and 60 – 80% centralities respectively). And experimental data in Ref.[23, 24] are shown as the filled patterns(0 – 5%, 30 – 40% and 70 – 80% centralities).

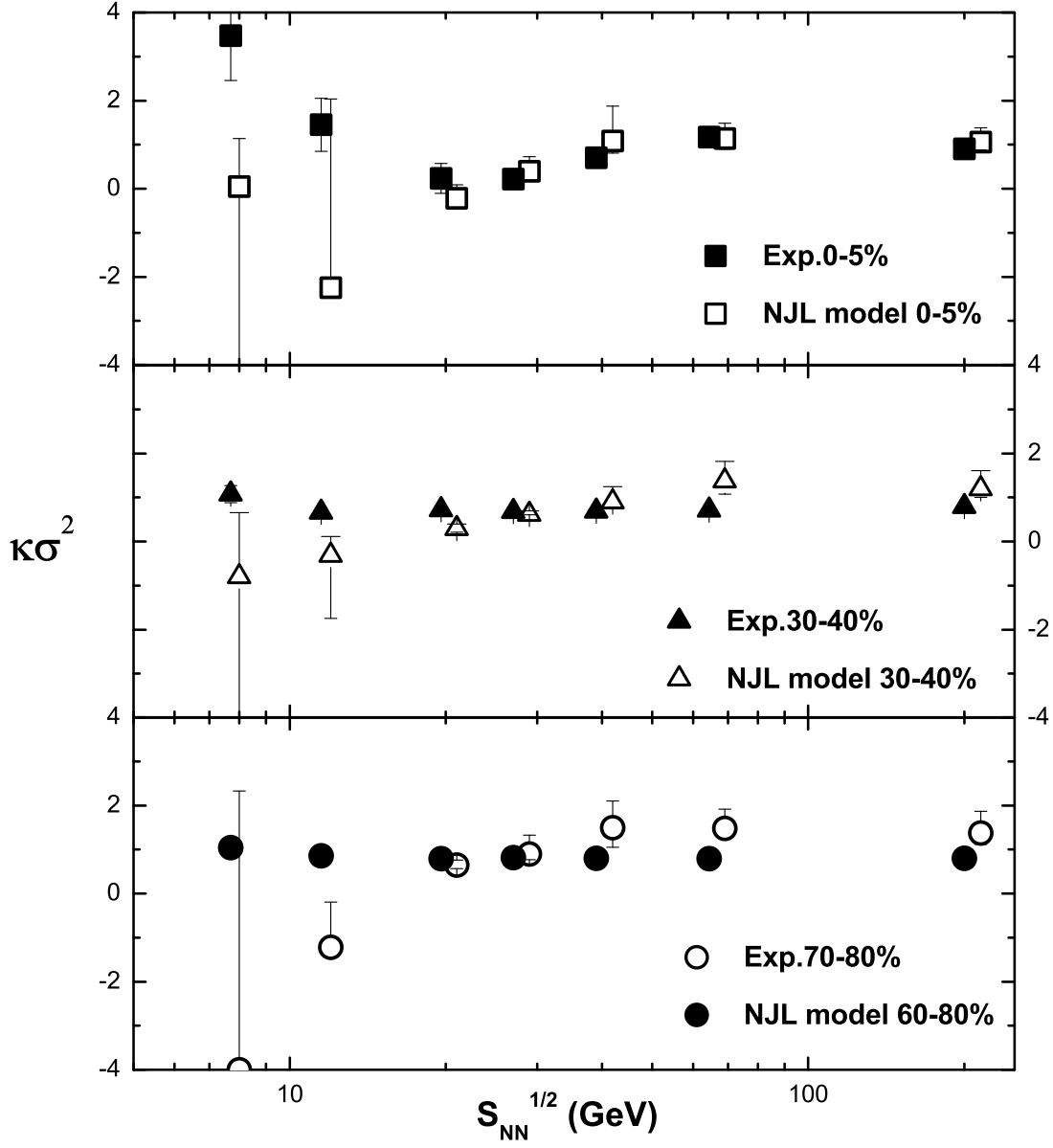


FIG. 3: $\kappa\sigma^2$ of the NJL model and the experiments. The NJL results demonstrate as empty squares, triangles and circles (0 – 5%, 30 – 40% and 60 – 80% centralities respectively). And experimental data in Ref.[23] are shown as the filled patterns (0 – 5%, 30 – 40% and 70 – 80% centralities).